# Single- and multi-shot laser-induced damages of $Ta_2O_5/SiO_2$ dielectric mirrors at 1064 nm

**Ying Wang (王 营)[1,2*], Hongbo He (贺红波)[1], Yuan'an Zhao (赵元安)[1], Yongguang Shan (单永光)[1,2], Dawei Li (李大伟)[1], and Chaoyang Wei (魏朝阳)[1]**

[1]*Key Laboratory of Materials for High Power Lasers, Shanghai Institute of Optics and Fine Mechanics, Chinese Academy of Science, Shanghai 201800, China*

[2]*Graduate University of the Chinese Academy of Sciences, Beijing 100049, China*

**Corresponding author: sdwangy@hotmail.com*

Received August 27, 2010; accepted November 3, 2010; posted online January 28, 2011

$Ta_2O_5/SiO_2$ dielectric mirrors deposited by ion beam sputtering (IBS) are studied. The multi-shot laser-induced damage threshold (LIDT) and its dependence on the number of shots are investigated, after which we find that the multi-shot LIDT is lower than that of single-shot. The accumulation effects of defects play an important role in the multi-shot laser damage. A simple model, which includes the conduction band electron production vsa multiphoton and impact ionizations, is presented to explain the experimental phenomena.

*OCIS codes:* 310.6870, 140.3330, 230.4040, 230.4170

*doi: 10.3788/COL201109.023103.*

In recent years, multi-shot laser-induced damage on optical materials, such as potassium dihydrogen phosphate (KDP) crystal, fused silica, and multilayer coating, has become a popular research topic. Multi-shot laser induced damage threshold (LIDT) has often been shown to be much lower than that of single-shot because of the accumulation effects[1−4]. In order to understand the mechanism of the multi-shot laser damage of the optical multilayer used in high-power laser systems, we attempt to find the correlations between observed laser damage threshold and the number of shots. The mechanism for single-shot laser damage includes avalanche ionization[5], multi-photon ionization[6], and impurity breakdown[7]. However, the damage mechanism of multi-shot radiation is more complicated than that of single-shot radiation. The mechanism of multi-shot damage has not been fully understood yet, which obviously has a very important impact on the practical applications of optical systems. In the femtosecond regime, the damage is intrinsic; in contrast, defects or impurities have been shown to play an important role in the laser-induced damage in the nanosecond regime[8]. The aim of this letter is to analyze the accumulation effects on the laser damage resistance in nanosecond regime and find correlations between observed LIDT and the number of shots.

In this letter, we present the results of 1-on-1 and $S$-on-1 tests at 1064 nm in $Ta_2O_5/SiO_2$ dielectric mirrors. Then, we give the experimental details concerning the sample deposition process and the laser damage test procedure. Finally, the experimental results and discussions are also given.

The mirror coatings were prepared by ion beam sputtering. The coating design of the sample was G $|(HL)^{13}H|$A. Here, H denoted high index material $Ta_2O_5$ with one quarter wavelength optical thickness (QWOT), L denoted low index material $SiO_2$ with one QWOT, G denoted BK7 substrate, and A denoted the incident medium (air). The transmittance spectrum of the sample is shown in Fig. 1.

The experimental setup for laser damage is shown schematically in Fig. 2, in which the Nd:YAG laser system operated at the $TEM_{00}$ mode and the pulse width was 12 ns at 1064 nm. The laser was focused to provide a far-field circular Gaussian beam. The effective area of the spot on the sample was 0.12 $mm^2$, which was measured by a laser beam analyzer. In the $S$-on-1 test, the sample was tested at the frequency of 5 Hz. The laser energy used to damage the sample was obtained by adjusting the attenuator, after which the pulse energy was measured by an energy meter from a split off portion of the beam. The sample was set upon a two-dimensional

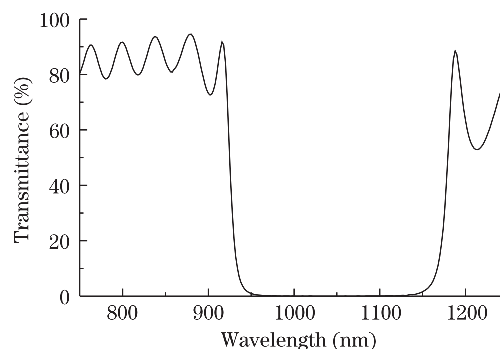


Fig. 1. Transmittance spectrum of the sample.

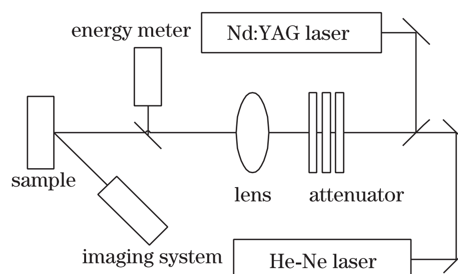


Fig. 2. Experimental setup of laser damage testing.

 © 2011 Chinese Optics Letters

precision stage driven by a stepper motor. The angle of incidence was slightly $2^\circ - 3^\circ$ off normal to avoid interference effects due to reflection from the substrate exit surface. The He-Ne laser was used to monitor the test, and damage onset was detected on-line by a video microscopy system.

The LIDT of the samples was tested in 1-on-1 and $S$-on-1 at 1064 nm according to ISO 11254-1[9] and ISO 11254-2[10]. Here, ten sample sites were exposed at the same fluence, and this procedure was repeated until the range of fluences was sufficiently broad to include points of 0–100% damage probability; this was done to develop a plot of damage probability versus fluence. The LIDT is defined as the energy density of the incident pulse when the damage occurs at 0% damage possibility (J/cm$^2$); it could be obtained by linear extrapolation of the damage probability data to zero damage probability. In this letter, 1-on-1, 10-on-1, 50-on-1,100-on-1, and 1000-on-1 LIDTs were tested to understand the influence of shot number on the accumulation effects.

The LIDT of the samples at 1064 nm for single- and multi-shot tests are summarized in Fig. 3, in which multi-shot LIDT is lower than that of the single-shot LIDT, and LIDT depends on the laser shot number. The multi-shot LIDT decreases with the increasing shot number, and this is leveled off when the fluence reaches a certain value.

There are several kinds of mechanisms for the multi-shot damage, such as heating inclusion model, band-breaking model, and colored center model[11]. In general, the damage fluence decreasing from the single-shot value to a certain value can be considered as the endurance limit of the optical surface in the multi-shot damage behavior[10]. The damages often originate from defects for both single and multi-shot tests at the nanosecond regime in a low frequency[12,13]. The multi-shot damage has been considered as the cause of the irreversible changes of optical properties of defects and ambient material[14,15]. The accumulation of irreversible changes can lead to the multi-shot LIDT, which is lower than the single-shot LIDT[16].

Due to the interference effects in film, local intensity enhancements exist in the sample coatings. The theoretical results of electric field distributions of the sample are calculated using thin film design software (TFCalc) (Fig. 4). Damages of the $Ta_2O_5/SiO_2$ dielectric mirrors most likely occur at the first interface between $Ta_2O_5$ and $SiO_2$, where has the maximum standing-wave electric field intensity[17]. Moreover, the band gaps of bulk materials $SiO_2$ and $Ta_2O_5$ are 7.8 and 4.6 eV[18], respectively.

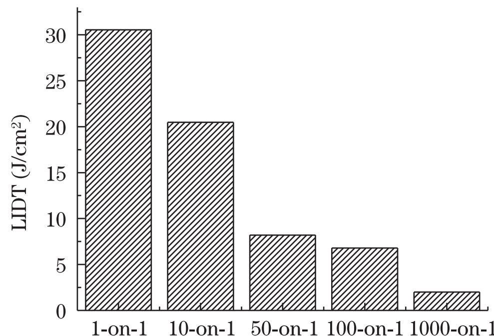


Fig. 3. LIDT results of the samples.

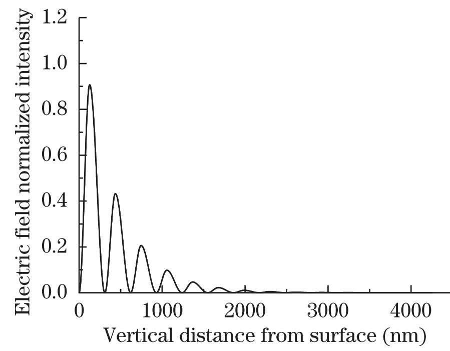


Fig. 4. Electric field intensity profile in $Ta_2O_5/SiO_2$ HR coating normalized to the incident electric field value at the wavelength of 1064 nm.

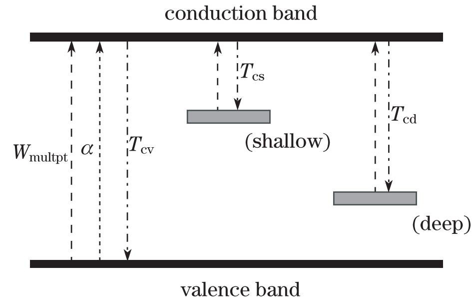


Fig. 5. Diagram of energy level in the wide gap dielectric materials.

With the excitation wavelength of 1064 nm, $Ta_2O_5$ must absorb fewer photons than $SiO_2$; thus, the damage would likely occur in the high index $Ta_2O_5$ layer first.

The conduction band electron density can be described by the general equation[6,19]

$$\frac{\mathrm{d}N}{\mathrm{d}t} = \eta(E)N(t) + \left(\frac{\mathrm{d}N}{\mathrm{d}t}\right)_{\mathrm{PI}} - \left(\frac{\mathrm{d}N}{\mathrm{d}t}\right)_{\mathrm{loss}}, \quad (1)$$

where $N(t)$ is the free electron density, $\eta(E)$ is the probability per unit time for an electron to undergo an ionizing collision, and $E$ is the electric field strength. The second term on the right-hand side is the multiphoton ionization contribution, and the third term is the loss due to electron diffusion, recombination, etc.

Considering the accumulation effects of defects in the wide gap coating material combination of $Ta_2O_5/SiO_2$, the model proposed by Mero *et al.*[20] is adopted in the nanosecond damage regime. The defects can be considered as two types of midgap trapping states that serve as shallow and deep traps that can be native or laser-induced in the wide-band gap material. The shallow states represent the state within one photo energy of the conduction band, such as bandtail states[21], while the deep states represent the states representing the multi-photo energy of the conduction band, such as self-trapped excitons and color center (such as oxygen vacancies)[13]. The simplest energy diagram and processes of the model are illustrated in Fig. 5. The band-to-band transitions are represented by avalanche ionization, multiphoton absorption, and a relaxation mechanism. Electrons in the conduction band can relax to the valence band with a characterized time constant $T_{\mathrm{cv}}$, and the trapping rate of electrons from the conduction band is characterized by two time constants, $T_{\mathrm{cd}}$ and $T_{\mathrm{cs}}$, respectively.

The electron density in the conduction band is described by the following set of rate equations[20]

$$\frac{\mathrm{d}N}{\mathrm{d}t}=\alpha N(t)I(t)+W_{\mathrm{multpt}}-\frac{N(t)}{T_{\mathrm{cv}}}-\frac{N(t)}{T_{\mathrm{cs}}}\left[1-\frac{N_{\mathrm{s}}(t)}{N_{\mathrm{s,max}}}\right]+\sigma_{\mathrm{s}}N_{\mathrm{s}}(t)\left[\frac{I(t)}{h\nu}\right]-\frac{N(t)}{T_{\mathrm{cd}}}\left[1-\frac{N_{d}(t)}{N_{\mathrm{d,max}}}\right]+\sigma N\left[\frac{I(t)}{h\nu}\right]^{m'}, \quad (2)$$

$$\frac{\mathrm{d}N_{\mathrm{s}}}{\mathrm{d}t}=\frac{N(t)}{T_{\mathrm{cs}}}\left[1-\frac{N_{\mathrm{s}}(t)}{N_{\mathrm{s,max}}}\right]-\sigma_{\mathrm{s}}N_{\mathrm{s}}(t)\left[\frac{I(t)}{h\nu}\right]-\frac{N_{\mathrm{s}}(t)}{T_{\mathrm{sv}}}, \quad (3)$$

$$\frac{\mathrm{d}N_{\mathrm{d}}}{\mathrm{d}t}=\frac{N(t)}{T_{\mathrm{cd}}}\left[1-\frac{N_{\mathrm{d}}(t)}{N_{\mathrm{d,max}}}\right]-\sigma_{\mathrm{d}}N_{\mathrm{d}}(t)\left[\frac{I(t)}{h\nu}\right]^{m'}-\frac{N_{\mathrm{d}}(t)}{T_{\mathrm{dv}}}, \quad (4)$$

where $\alpha$ is the avalanche ionization coefficient; $N_{\mathrm{s}}$ and $N_{\mathrm{d}}$ are the number densities of shallow traps and deep traps, respectively; $N_{\mathrm{d,max}}$ and $N_{\mathrm{s,max}}$ are the maximum shallow trap and deep trap density, respectively; $\sigma_{\mathrm{s}}$ is the absorption cross-section of an electron in a shallow trap; $\sigma_{\mathrm{d}}$ is the multi-photon absorption cross- section of the deep traps. $I(t)$ is the laser intensity and is given by $I(t)=I_0\exp(-\frac{4ln2t^2}{\tau^2})$, where $I_0$ is the laser fluence and $\tau$ is the pulse duration. The multiphoton ionization (MPI) rate can be described using the theory of Keldysh[22] expressed by

$$W_{\mathrm{multpt}}=\frac{2w}{9\pi}\left(\frac{m^*w}{\hbar}\right)^{3/2}\Phi\sqrt{2\left\langle E_{\mathrm{g}}'/\hbar w\right\rangle-(2E_{\mathrm{g}}'/\hbar w)}\times\exp\left\{2\left\langle E_{\mathrm{g}}'/\hbar w\right\rangle\left(1-\frac{1}{4\gamma^2}\right)\right\}\left(\frac{1}{16\gamma^2}\right)^{\left\langle(E_{\mathrm{g}}'/\hbar w)+1\right\rangle}, \quad (5)$$

where $\gamma=w\sqrt{m_{\mathrm{e}}E_{\mathrm{g}}}/eE$, $E$ is the electric field oscillating at frequency $w$, $e$ denotes the electron charge, $E_{\mathrm{g}}'=E_{\mathrm{g}}\left[1+(1/2\gamma^2)\right]$ represents the effective band gap energy in the radiation field, $m^*=m_{\mathrm{e}}m_{\mathrm{h}}/(m_{\mathrm{e}}+m_{\mathrm{h}})$ indicates the reduced effective mass of the conduction electron and valence hole, $m_{\mathrm{h}}$ is the effective conductivity masses of holes, the symbol $\langle\cdot\rangle$ denotes the integer part, and $\Phi$ describes the Dawson function.

Between the pulses, the population numbers are described by the following rate equations[20]

$$\frac{\mathrm{d}N}{\mathrm{d}t}=-\frac{N(t)}{T_{\mathrm{cv}}}-\frac{N(t)}{T_{\mathrm{cs}}}\left[1-\frac{N_{\mathrm{s}}(t)}{N_{\mathrm{s,max}}}\right]-\frac{N(t)}{T_{\mathrm{cd}}}\left[1-\frac{N_{\mathrm{d}}(t)}{N_{\mathrm{d,max}}}\right], \quad (6)$$

$$\frac{\mathrm{d}N_{\mathrm{s}}}{\mathrm{d}t}=\frac{N(t)}{T_{\mathrm{cs}}}\left[1-\frac{N_{\mathrm{s}}(t)}{N_{\mathrm{s,max}}}\right], \quad (7)$$

$$\frac{\mathrm{d}N_{\mathrm{d}}}{\mathrm{d}t}=\frac{N(t)}{T_{\mathrm{cd}}}\left[1-\frac{N_{\mathrm{d}}(t)}{N_{\mathrm{d,max}}}\right]. \quad (8)$$

In this letter, the equations are solved numerically for a train of square pulses. Equations (2)–(4) are for the pulses that are on and Eqs. (6)–(8) are for the pulses that are off. The laser fluence required for damage at a given number of shot is determined repeatedly by integrating the system when the conduction band electron density surpasses a critical plasma density $N_{\mathrm{cr}}$, represented by[23] $N_{\mathrm{cr}}=\frac{\varepsilon_0 m^* w^2}{e^2}$, where $\varepsilon_0$ is the permittivity of free space.

**Table 1. List of Parameters for $Ta_2O_5$ and $SiO_2$**

| | $E_{\mathrm{g}}$(eV) | $n_0$ | $m^*$ | $m_{\mathrm{e}}$=$m_{\mathrm{h}}$ |
|---|---|---|---|---|
| $Ta_2O_5$ | 4.6 | 2.01 | 0.635 | 1.0 |
| $SiO_2$ | 7.8 | 1.43 | 0.635 | 1.0 |

*The values for $E_{\mathrm{g}}$ are obtained from a previous work[18]. The values for $m^*$, $m_{\mathrm{e}}$, and $m_{\mathrm{h}}$ are obtained from another work[24].

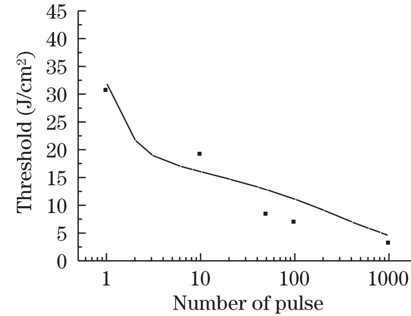


Fig. 6. Damage threshold as a function of the number of pulse. The dashed line is the result of simulations using the model based on Eqs. (2)–(8).

The values of all parameters included in Eqs. (2)–(8) are shown in Table 2. The quantities $N_{\mathrm{d,max}}$, $N_{\mathrm{s,max}}$, $\sigma_{\mathrm{d}}$, and $\sigma_{\mathrm{s}}$ are adjusted to match the experiment. The simulation results are shown in Fig. 6, in which the model explains the most important features of the experimental data. The LIDT decreases slowly until it levels off when the laser fluence reaches a certain value. It means that the shallow and deep traps are both saturated when the laser shot numbers reach a certain number. The electron numbers become balanced from the conduction band, the shallow and deep traps when the laser fluence reaches below a certain value.

If there is no change in optical properties of defects and ambient material, the laser damage probability of $S$-on-1 test should be the same as in the case of 1-on-1 test[25]. In other cases, an increase or decrease of the threshold means that under successive laser irradiations corresponding to the creation of laser-induced defects or modification of the defects structure, the laser-induced defects can be reversible and irreversible. When the irreversible laser-induced defects represent accumulation effects, the laser fluence below the single-shot LIDT can lead to damage in the multi-shot procedure.

The above analysis shows that the multi-shot laser damage is related to the irreversible changes of native or laser-induced defects in the multilayer. Moreover, the irreversible accumulated changes of laser-induced defects or native defects result in the decrease of multi-shot LIDT.

In conclusion, the multi-shot damage behavior of $Ta_2O_5/SiO_2$ dielectric mirrors is studied experimentally and theoretically. Accumulation effects play an important role in the multi-shot laser damage of HR at 1064 nm. The decrease of the damage threshold is caused by the irreversible accumulated changes of the laser-induced defects or native defects. A simple model involving the conduction band electron is used to explain the experimental result. The relation of LIDT for the coatings in calculation agrees with the experimental result.

## References


1. S. C. Jones, P. Braunlich, R. T. Casper, X. A. Shen, and P. Kelly, Opt. Eng. **28,** 1039 (1989).
2. A. A. Manenkov and V. S. Nechitailo, Proc. SPIE **1441,** 392 (1991).
3. J. Y. Natoli, B. Bertussi, and M. Commandre, Opt. Lett. **30,** 1315 (2005).
4. Y. Zhao, Z. Tang, J. Shao, and X. Fan, Proc. SPIE **5273,** 23 (2004).
5. A. S. Epifanov, Quantum Electron. **17,** 2018 (1981).
6. N. Bloembergen, Quantum Electron. **10,** 375 (1974).
7. R. W. Hopper and D. R. Uhlmann, Appl. Phys. **41,** 4023 (1970).
8. X. Li, Y. Zhao, X. Liu, J. Shao, and Z. Fan, Chin. Opt. Lett. **8,** 615 (2010).
9. International Organization for standardization, ISO11254-1, Lasers and laser-related equipment - determination of laser-induced damage threshold of optical surfaces-Part 1 (2000).
10. International Organization for standardization, ISO11254-2, Lasers and laser-related equipment-determination of laser-induced damage threshold of optical surfaces-Part 2 (2000).
11. A. E. Chmel, Materials Science and Engineering **49,** 175 (1997).
12. T. Wang, Y. Zhao, J. Huang, H. He, J. Shao, and Z. Fan, Acta Photon. Sin. **35,** 859 (2006).
13. Y. N. Zhao, Y. J. Wang, H. Gong, J. D. Shao, and Z. X. Fan, Appl. Sur. Sci. **210,** 353 (2003).
14. M. F. Koldunov, A. A. Manenkov, and I. L. Pocotilo, Proc. SPIE **2428,** 653 (1995).
15. Y. Zhao, W. Gao, J. Shao, and Z. Fan, Appl. Sur. Sci. **227,** 275 (2004).
16. L. A. Emmert, M. Mero, and W. Rudolph, Appl. Phys. **108,** 043523 (2010).
17. L. Yuan, Y. N. Zhao, C. J. Wang, H. B. He, Z. X. Fan, and J. D. Shao, Appl. Sur. Sci. **253,** 3450 (2007).
18. N. Liu, Y. J. Wang, M. Zhou, X. F. Jing, Y. Z. Wang, Y. Cui, and Y. X. Jin, Chin. Phys. Lett. **27,** 074215 (2010).
19. D. Du, X. Liu, G. Korn, J. Squier, and G. Mourou, Appl. Phys. Lett. **64,** 3071 (1994).
20. M. Mero, L. A. Emmert, and W. Rudolph, Proc. SPIE **7132,** 713209 (2008).
21. L. A. Emmert, D. Nguyen, M. Mero, W. Rudolph, D. Patel, E. Krous, and C. S. Menoni, in *Proceedings of 2009 Conference on Lasers and Electro-Optics and Quantum Electronics and Laser Science* CTuEE5 (2009).
22. L. V. Keldysh, J. Exptl. Theovet. Phys. **20,** 1307 (1965).
23. K. Starke, D. Ristau, H. Welling, T. V. Amotchkina, M. Trubetskov, A. A. Tikhonravov, and A. S. Chirkin, Proc. SPIE **5273,** 501 (2004).
24. L. Sudrie, A. Couairon, M. Franco, B. Lamouroux, B. Prade, S. Tzortzakis, and A. Mysyrowicz, Phys. Rev. Lett. **89,** 186601 (2002).
25. J. Capoulade, L. Gallais, J. Y. Natoli, and M. Commandre, Appl. Opt. **47,** 5272 (2008).